Chinese Chemical Letters 34 (2023) 108184

Contents lists available at ScienceDirect

Chinese Chemical Letters

journal homepage: www.elsevier.com/locate/cclet

Targeting self-enhanced ROS-responsive artesunatum prodrug nanoassembly potentiates gemcitabine activity by down-regulating CDA expression in cervical cancer

Shengtao Wang[a,b,1], Kunyi Yu[b,1], Zhiyu Yu[b,1], Bingchen Zhang[b,c], Chaojie Chen[b], Ling Lin[b], Zibo Li[b], Zhongjun Li[c,*], Yuhua Zheng[a,**], Zhiqiang Yu[b,c,*]

[a] *Affiliated Foshan Maternity & Child Healthcare Hospital, Southern Medical University (Foshan Maternity & Child Healthcare Hospital), Foshan 528000, China*

[b] *School of Pharmaceutical Sciences, Southern Medical University, Guangzhou 510515, China*

[c] *Department of Obstetrics and Gynecology, Affiliated Dongguan Hospital, Southern Medical University, Dongguan 523059, China*

ARTICLE INFO

Article history:
Received 24 November 2022
Revised 25 December 2022
Accepted 31 January 2023
Available online 7 February 2023

Keywords:
ROS self-supplied
ROS-responsive
Self-delivery carrier
Down regulation of CDA
Synergistic anti-tumor effect
Cervical cancer

ABSTRACT

Prodrug self-delivery carriers with targeting that specifically responded to tumor microenvironments have good potential to improve the application dilemma of approved clinical therapeutic drugs (systemic distribution and side effects). It's noted the conversion of gemcitabine (GEM) to inactive ingredients under the action of cytidine deaminase (CDA) during metabolism *in vivo* limits its clinical effect. A high level of reactive oxygen species (ROS) results in a high level of oxidative stress in tumor cells, which changes the expression of CDA and optimizes the metabolism of GEM *in vivo* and overcome drug resistance. In this study, the ROS responsive and ROS self-supplied prodrug of artemisia (ART)-thioacetal bond (TK)-GEM was synthesized and self-vectors based on ART-TK-GEM (TK@FA NPs) was prepared by using nano precipitation. ROS responsive characteristics ensure specific release of prodrugs in tumor cells with high level of ROS thereby reducing side effects on normal cells and tissues. The endogenous ROS and newly generated ROS by ART can reduce the expression of CDA and optimizes the metabolism of GEM, and the accumulated ROS can also induce apoptosis of tumor cells, realizing synergistic anti-tumor effect of chemical drugs and traditional Chinese medicines. This paper proposes a simple method by using clinically approved drugs to improve the insufficient effect of existing chemotherapy and overcome resistance, which has potential to appropriately shorten the drug development cycle and accelerate the clinical investigation of drugs.

Chemotherapy is an effective means of tumor treatment in clinic, but its obvious side effects on normal tissues due to the systemic distribution of drugs makes patients face serious health recovery, psychological and economic burdens [1–5]. Drug nanocrystalization provides a strategy to improve drug biodistribution and reduce side effects on normal tissues so as to achieve effective drug enrichment in tumor tissues and efficient inhibition of tumor growth [1,2,6]. Vector-free or drug self-carrier delivery systems, a method for drug nanocrystallization, have significant advantages over traditional nanocarriers (liposomes, micelles, albumin and polymers), such as higher drug loading ability and biosafety, lower health recovery and psychological burden [4,7–9]. Homodimer or hetero-dimer of chemotherapeutic drugs with special sensitive bonds have been proved to form vector-free or drug self-carrier delivery systems, receiving wide attention from researchers [10–12]. Prodrugs that respond specifically to tumor microenvironments (TME), such as high levels of reactive oxygen species (ROS) and glutathione (GSH), can achieve specific drug killing of tumor cells and reduce toxic side effects on normal tissues [13–17]. The unique physiological characteristics of tumor cells endows them special receptors on the surface of tumor cells that are different from those of normal cells, which can be used to design tumor specific targeting vector. Folic acid (FA) receptor (FR) is a promising anticancer drug target owing to the overexpression of FR in ovarian, lung and breast cancers. Targeting vectors specifically recog-

* Corresponding authors at: Department of Obstetrics and Gynecology, Affiliated Dongguan Hospital, Southern Medical University, Dongguan 523059, China.
** Corresponding author.
E-mail addresses: Zhongjun@gdmu.edu.cn (Z. Li), zyh2013916@163.com (Y. Zheng), yuzq@smu.edu.cn (Z. Yu).
[1] These authors contributed equally to this work.

https://doi.org/10.1016/j.cclet.2023.108184
1001-8417/

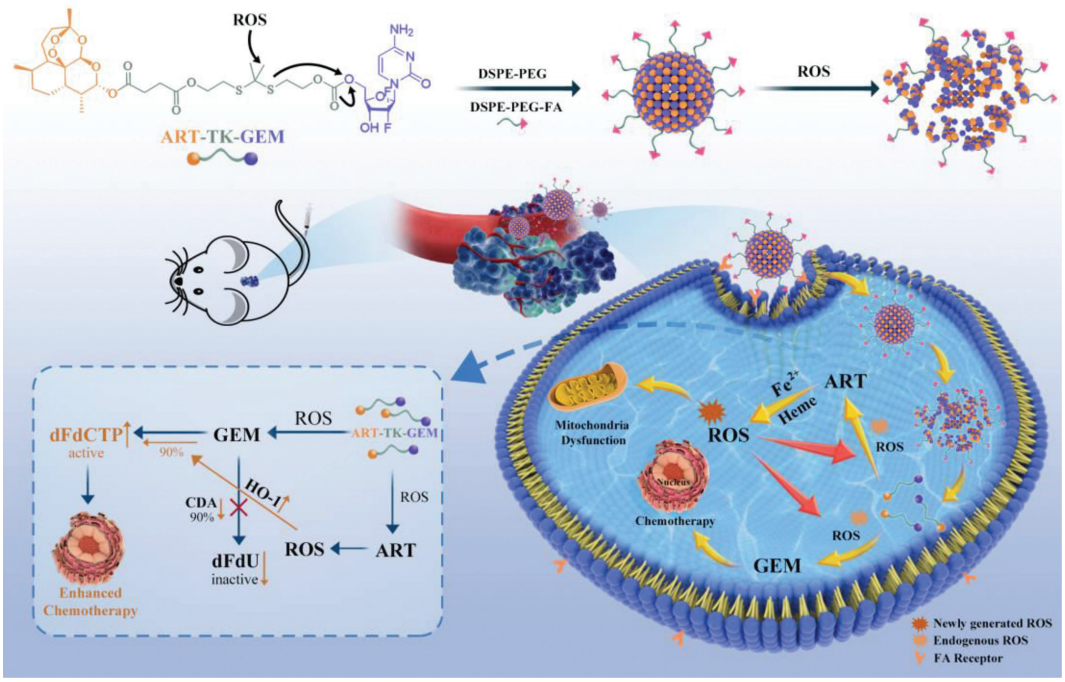

Scheme 1. The preparation of targeting nanomedicine based on ROS responsive traditional Chinese medicine prodrugs for synergistic and enhanced chemotherapy.

nized by tumor cells can further improve the enrichment of drugs in tumor sites and reduce toxic and side effects [18–21]. To some extent, prodrug self-delivery carriers with targeting and responding specifically to TME have good potential to effectively improve the application dilemma of approved clinical therapeutic drugs.

Gemcitabine (GEM) is a clinically approved drug for the treatment of a variety of tumors, but GEM inactivating enzyme (cytidine deaminase, CDA) in tumor cells limits its antitumor properties and GEM also has all the problems associated with free chemotherapeutic drugs mentioned above [22,23]. Previous studies have found that the expression level of CDA in tumor cells is closely related to the level of cellular oxidative stress. High oxidative stress level can significantly reduce the expression level of CDA, which is conducive to the transformation of GEM into active ingredient to improve the anti-tumor effect of GEM [24–28]. ROS-producing drugs, such as paclitaxel [24,25,27], photosensitizers [4,5,29,30] and artemisia annul analogues [31,32], have been proved to break the redox balance of tumor cells and produce high oxidative stress, further increasing the expression of heme oxygenase-1 (HO-1), and the high expression of HO-1 have potential to inhibit the expression of CDA [27,28]. However, researchers only load the two drugs together in one carrier, without introducing the concept of self-delivery carrier or designing chemotherapeutic drugs as response prodrugs to TME. Artemisia annua analogues are the widely used plant-derived traditional Chinese medicine, cheap and readily available. The unique peroxide bridge structure of artemisia annua analogues was opened by iron ion to produce ROS and endow them excellent anti-malarial properties and limit anti-tumor properties [31–35]. ROS produced by artemisia annua analogues is independent of external light sources [31,32] and they are clinically approved drugs, which is superior to photosensitizers and has a better application potential in the treatment of deep tumors.

Although heterodimers based on artemisia annua analogues and chemotherapeutic drugs have been reported, there is a lack of necessary analysis and explanation about the synergistic mechanism [36]. In this study, heterologous dimers of artesunatum (ART) and GEM with ROS responsive release characteristics (ART-TK-GEM) were designed and synthesized (Scheme 1 and Figs. S1–S3 in Supporting information). Relatively high levels of ROS (endogenous ROS) in tumor cells can break ROS-responsive thioacetal bonds, releasing free GEM and ART. ART can produce ROS (newly generated ROS) under the action of heme in mitochondrion, which can accelerate the break of thioacetal bond (TK) to release more ART, and the released ART can produce more ROS to achieve efficient release of GEM and ART and effective enrichment of ROS. The high level of ROS also inhibits the expression of CDA by upregulating the expression of HO-1, so that more GEM is converted into active ingredients and anti-tumor properties of GEM is improved. Under the synergy of ART and GEM, better anti-tumor effects of prodrug self-delivery carriers with targeting were achieved. This study potentially provides a new idea for drug development and drug optimization by strategically integrating clinically approved drugs that have synergistic effects. However, the ratio of ART and GEM was fixed in 1:1 in the dimeric prodrug, so the optimal synergistic treatment effect may be difficult to achieve. In future, other kinds of linker such as 2-amino-1,3-propanediol (serinol) or tromethamine (THAM) might be used to obtain heterologous prodrug with the ratio in 1:2 and 1:3 or in 2:1 and 3:1 and explore the synergistic treatment effect of different kinds of drugs including ART and GEM.

First, the ART-TK-GEM was synthesized in Fig. S1 according to previous literatures [37,38]. Briefly, the thioketal linker was first obtained [37,38] and reacted with ART to give compound ART-TK. Next, ART-TK was reacted with 4-nitrophenyl chloroformate through esterification reaction to give ART-TK-Nitrone. Then ART-TK-Nitrone was reacted with GEM to obtain ART-TK-GEM. The structure of ART-TK-GEM was confirmed by electro spray ionization-mass spectroscopy (ESI-MS) and nuclear magnetic resonance (NMR) (Figs. S2 and S3).

As known, the TK linker was ROS-cleavable and original drug could be released *via* an intramolecular reaction triggered by ROS generated by ART or photosensitizers [37,38]. To confirm that, ART-TK-GEM was treated with different concentration of H_2O_2, and then the solution was analyzed with high performance liquid chromatography (HPLC) (Fig. 1A). It was found that a new peak at 3 min

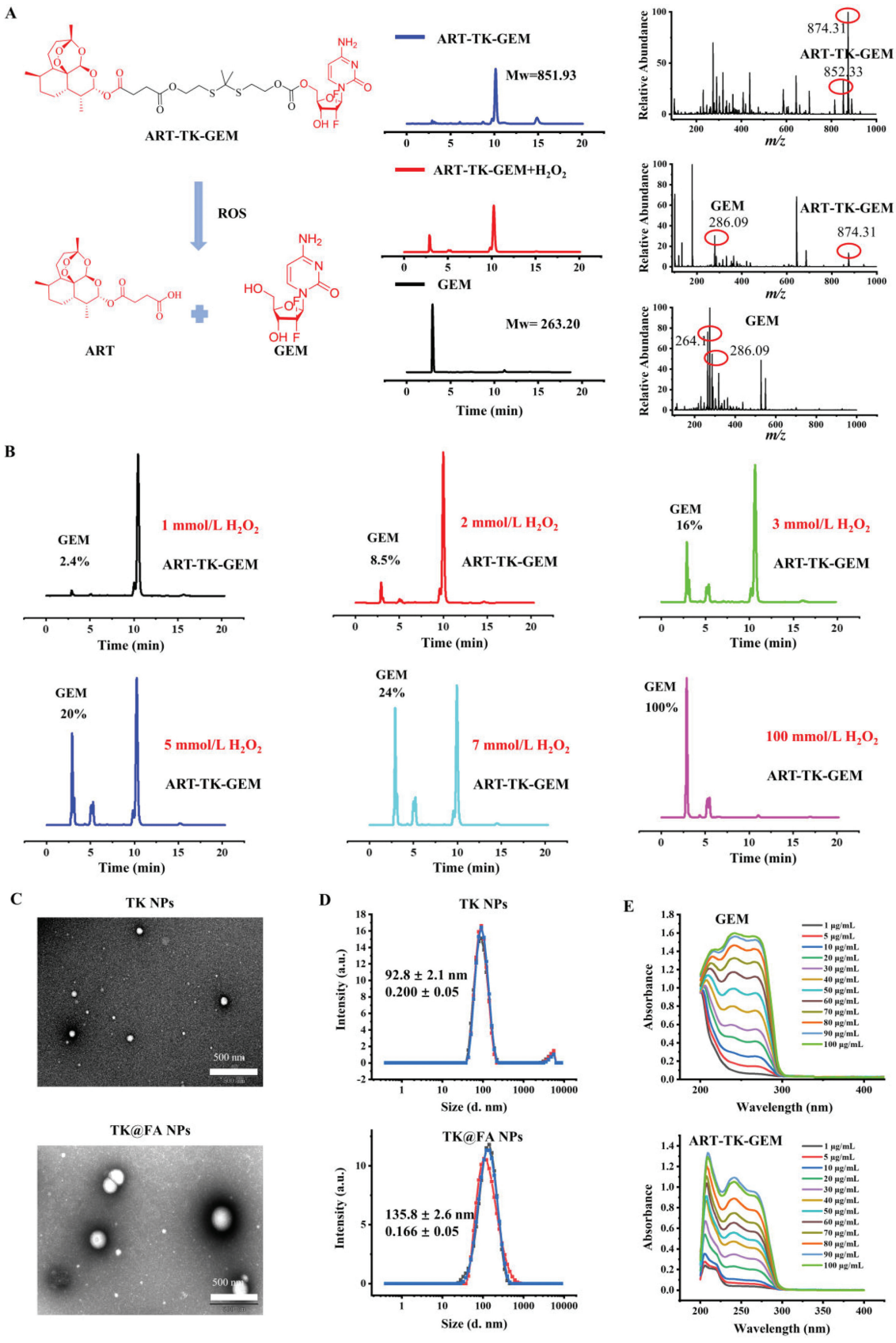

Fig. 1. Characterization of prodrugs and prodrug nanoparticles. (A) The synthesis route of ART-TK-GEM. (B) The ROS-activated drug release performance of ART-TK-GEM. (C, D) The TEM images (C) and dynamic light scattering (DLS) (D) of TK NPs and TK@FA NPs. (E) The UV–vis spectrum of GEM and ART-TK-GEM.

appeared, which was consist with the elution time of free GEM, indicating that GEM as released after the treatment of H_2O_2. Meanwhile, the peak of ART-TK-GEM at 10.2 min decreased obviously, suggesting GEM was released efficiently triggered by ROS. The TK linker could be broken at 1 mmol/L concentration of H_2O_2 and as more H_2O_2 was added, more GEM was released (Fig. 1B). The liquid chromatography-mass spectrometry (LC-MS) further confirmed that TK linker was ROS-cleavable and original drug GEM was released (Fig. 1B).

Drug nanocrystalline had been proved to be an effective method to improve drug efficacy and reduce drug side effects. Vector free and drug self-carrier delivery systems had been shown to significantly increase loading capacity and improve the biosafety of drug delivery systems. Some kinds of drug homologous dimers and heterologous dimers also showed the potential of nanocrystallization under a series of intermolecular forces due to the difference in hydrophilicity of drug fragments. As a kind of drug heterologous dimer, ART-TK-GEM formed nanoparticles with the size of 92.8 ± 2.1 nm (TK NPs) and 135.8 ± 2.6 nm (TK@FA NPs) by nanoprecipitation from tetrahydrofuran (THF) to water under the action of intermolecular forces. As reported, distearoyl phosphoethanolamine-PEG_{2000} (DSPE-PEG_{2k}) and DSPE-PEG_{2k}-FA was used to improve the stability of assemblies of drug homologous dimers and heterologous dimers, because amphiphilic DSPE-PEG was involved in the self-assembly of prodrug and inserted into the assemblies. The transmission electron microscope (TEM) image of the NPs revealed smaller dimeter, likely due to shrinkage during sample preparation (Figs. 1C and D). The TK NPs and TK@FA NPs were stable, and no significant size change was found for 28 days in phosphate buffered saline (PBS) and PBS with 10% fetal bovine serum (FBS) (Fig. S4 in Supporting information). The ultraviolet–visible spectroscopy (UV–vis) spectrum of GEM and ART-TK-GEM was shown in Fig. 1E and the characteristic peak of GEM in UV absorption had not significant change.

The endocytosis effect of nanoparticles by HeLa cells was evaluated by using confocal laser scanning microscope (CLSM) and flow cytometry. The fluorescent dye Ce 6 was used to trace the nanoparticles and two kinds of nanoparticles loaded with Ce 6 (Ce 6@TK NPs and Ce 6@TK@FA NPs) were obtained. As shown, the fluorescence of free Ce 6 was higher than that of Ce 6@TK NPs and Ce 6@TK@FA NPs a 4 h, indicating that free Ce 6 was more easily to enter the cells. Due to drug metabolism and continuous accumulation of nanoparticles, the fluorescence intensity of nanoparticles was stronger than that of free Ce 6 at 12 h (Fig. S5A in Supporting information). The data of fluorescence activated cell sorting (FACS) experiments also had the similar experimental results (Fig. S5C in Supporting information). The intracellular ROS level was determined by using 2′,7′-dichlorofluorescin diacetate (DCFH-DA) as a fluorescence probe through CLSM and FACS [4]. For the PBS group, only negligible green fluorescence was observed. For ART, ART+GEM and TK@NPs, bright green fluorescence was observed indicating that the peroxide bridge of ART could produce ROS catalyzed by heme in cells. TK@FA NPs had the brightest green fluorescence (Fig. S5B in Supporting information). The prodrug could produce sufficient ROS without light condition, which helps to overcome the deficiency of light dependence. Additionally, the quantitative intracellular ROS level was measured by using flow cytometry, as shown in Fig. S5D in Supporting information.

In response to endogenous ROS, prodrug nanoparticles (TK@NPs and TK@FA NPs) released GEM and ART, and the newly generated ROS produced by released ART under the action of Heme and Fe^{2+} ulteriorly accelerated the rupture of prodrugs and the release of free drugs. Under the synergistic action of endogenous ROS and newly generated ROS, effective fracture of prodrug and efficient release of the original drug achieved. Only when GEM was transformed into active ingredient (dFdCTP) could it play an effective role in tumor inhibitory, but when GEM was transformed into inactive ingredient (dFdU) through CDA, the tumor inhibition effect of GEM was limited [22,23,39]. It had been demonstrated that high level of ROS could increase the expression of HO-1 and high-level expression of HO-1 could inhibit the expression of CDA, promoting the conversion of GEM to active component (dFdCTP) and increasing the tumor inhibitory efficiency of GEM (Fig. S6A in Supporting information). Next, the *in vitro* cytotoxicity of the TK@NPs and TK@FA NPs compared with that of free ART and ART+GEM was evaluated by measuring half maximal inhibitory concentration (IC_{50}) of cell proliferation by using MTT method in HeLa cells after a 48-h treatment. By comparing free drug (ART and ART+GEM) and prodrug nanoparticles (TK@NPs and TK@FA NPs), the *in vitro* potency of the prodrug nanoparticles will be reduced due to the lower endocytosis efficiency and additional requirement of cleavage of the sulfur ketal to form free GEM. As shown (Fig. S6B in Supporting information), compared with free ART+GEM, TK@NPs and TK@FA NPs exhibited dose-dependent toxicity but were less toxic in a range of concentration, which was consistent with expectation (Fig. S6B). Double staining of calcein-AM/PI in HeLa cells also showed a similar result (Fig. S6C in Supporting information). To further evaluate the *in vitro* cytotoxicity of TK@NPs and TK@FA NPs, the cell apoptosis of HeLa was investigated by FACS after 48 h of treatment. As shown in Fig. S6D (Supporting information), the apoptotic ratios of ART+GEM, TK@NPs and TK@FA NPs were higher than that of free GEM, indicating ART could obviously enhance the antitumor effect of GEM.

It had been reported that up-regulation of HO-1 could inhibit the expression of CDA and then improved the antitumor properties of GEM. It was subsequently elucidated whether the increased inhibition of cell growth by ART+GEM, TK@NPs and TK@FA NPs than GEM was a consequence of increased HO-1 expression and decreased CDA expression. First, immunocytofluorescence assay was performed on HeLa cells and the antibody of CDA and HO-1 were stained with secondary antibodies labeled with red and green fluorescence, respectively. As shown in Fig. 2A, the expression of CDA obviously decreased and the expression of HO-1 obviously increased in HeLa cells after treating with ART+GEM, TK@NPs and TK@FA NPs. GEM metabolism might lead to decrease expression of CDA, and exogenous ROS produced by ART up-regulated expression of HO-1, further leading to decrease expression of CDA. The immune-fluorescence staining of tumor tissues and Western blot analysis of HeLa cells also shown the similar results (Figs. 2B and C). Based on the above results, it was believed that the improvement of anti-tumor properties of GEM was due to the down-regulation of CDA caused by the up-regulation of HO-1, and more GEM was converted into active ingredient (not proved in this paper) [24].

The enrichment ability and degree of nanodrugs in tumor sites determined the tumor inhibition properties and biosafety of nanodrugs, so the distribution property and targeting ability of TK@NPs and TK@FA NPs *in vivo* was evaluated on HeLa cells tumor-bearing BALB/c mice. Two kinds of nanoparticles loaded with ICG were prepared (ICG@TK@NPs and ICG@TK@FA NPs) and the fluorescence intensity *in vivo* at different time points was compared. For free ICG group, only negligible fluorescence was observed at tumor site at 24 h and obvious fluorescence could be observed at tumor site for ICG@TK@NPs and ICG@TK@FA NPs (Fig. S7A in Supporting information), indicating the nanocrystalization of ART-TK-GEM and DSPE-PEG could significantly enhanced the blood circulation time and improve its enrichment at the tumor site over a longer time. The quantitative assay of fluorescence intensity at tumor site (Fig. S7B in Supporting information) proved that nanoscale ART-TK-GEM could accumulated at the tumor site for a longer time than free ART-TK-GEM. The fluorescence signal of ICG@TK@FA NPs was higher than that of ICG@TK@NPs due to the

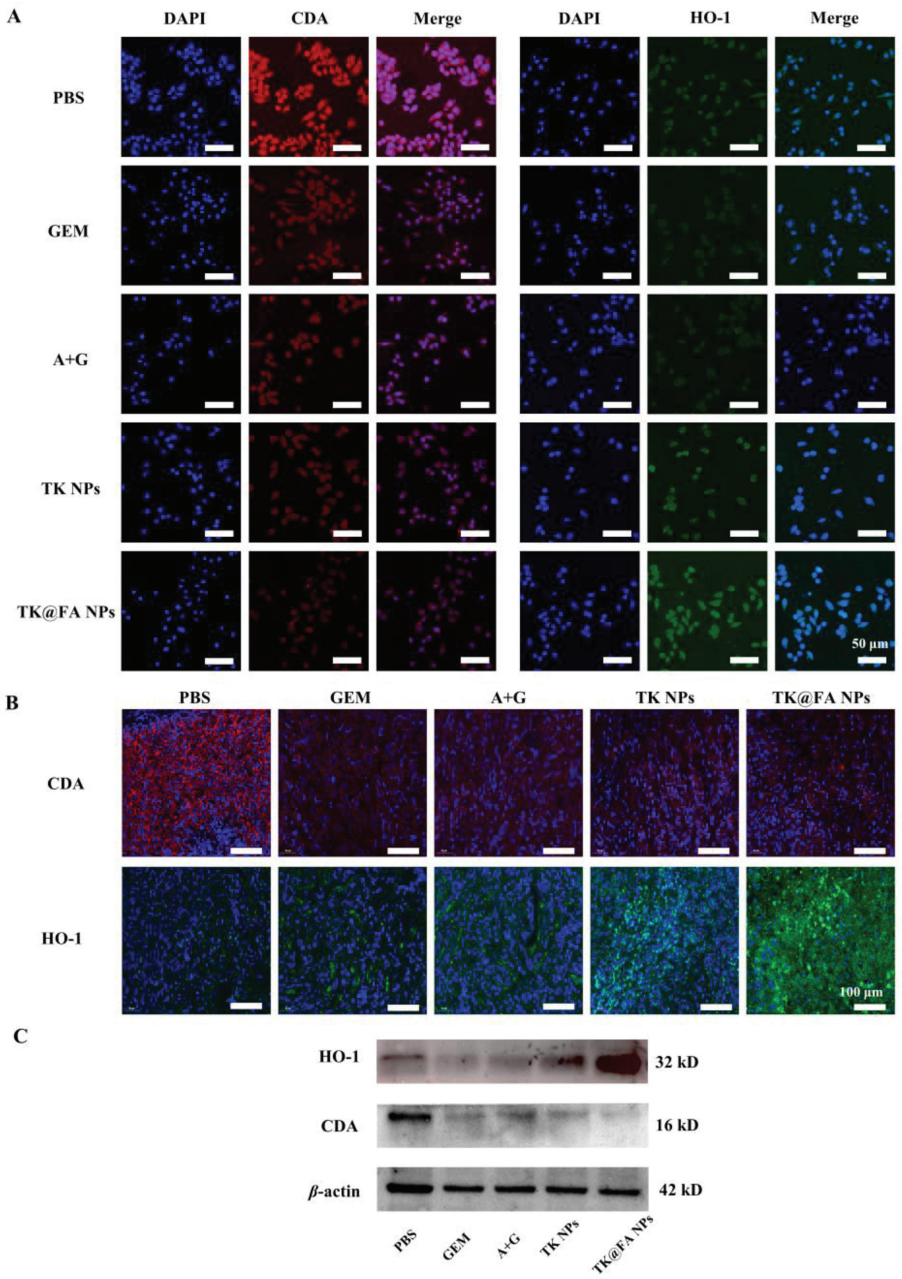

Fig. 2. Possible mechanisms by which ART enhances the antitumor effect of GEM. (A) Immunocytofluorescence to determine the expression of CDA (red) and HO-1 (green) in HeLa cells after incubating with GEM, ART+GEM (A + G), TK NPs and TK@FA NPs at 20 μmol/L (GEM-equivalent concentration) for 24 h. (B) Immunohistochemistry staining to determine the expression of CDA (red) in relation to the oxidative stress marker, HO-1 (green) for tumor tissues obtaining from HeLa tumor-bearing BALB/c nude mice after treatment for 21 days. (C) Western blot analysis of CDA and HO-1 expression after incubating with GEM, ART+GEM, TK NPs and TK@FA NPs at 20 μmol/L (GEM-equivalent concentration) for 24 h in HeLa cells. DAPI: 2-(4-Amidinophenyl)−6-indolecarbamidine dihydrochloride.

good targeting ability of FA to the FA receptor on the surface of cell membrane. Additionally, the fluorescence intensity of the major organs (Fig. S7C in Supporting information) showed that, in addition to the tumor sites, the nanoparticles were mainly distributed in the liver and kidney tissues, indicating that the nanoparticles were mainly metabolized by the liver and kidney. The quantitative fluorescence intensity of the tumors and major organs were shown in Fig. S7D (Supporting information).

Based on above results, the HeLa tumor-bearing BALB/c nude mice were selected to evaluate the anti-cancer efficiency of the prodrug NPs. All animal experiments were approved by Institutional Animal Care and Use Committee (IACUC) of Southern Medical University. The whole treatment process was shown in Fig. 3A. As shown in Fig. 3C, the tumor volume of PBS group grew quickly. For the group treatment with GEM, the increase of tumor volume was inhibited but only with limited inhibitory effect, implying that chemotherapy of GEM alone was insufficient in inhibiting tumor growth. The tumor inhibitory efficiency of ART+GEM and TK NPs were better than that of GEM, due to the antitumor effect of ART itself and ART could also enhance the anti-tumor effects of GEM. Notably, TK@FA NPs had higher antitumor efficiency than that of other groups owing to the antitumor effect of ART itself and better tumor enrichment of TK@FA NPs. The photographs of the tumors and tumor weight were shown in Figs. 3D and E. No obvious body weight changes were observed, indicating that prodrug NPs had no serious side effects (Fig. 3B). The Hemolysis test and blood bio-

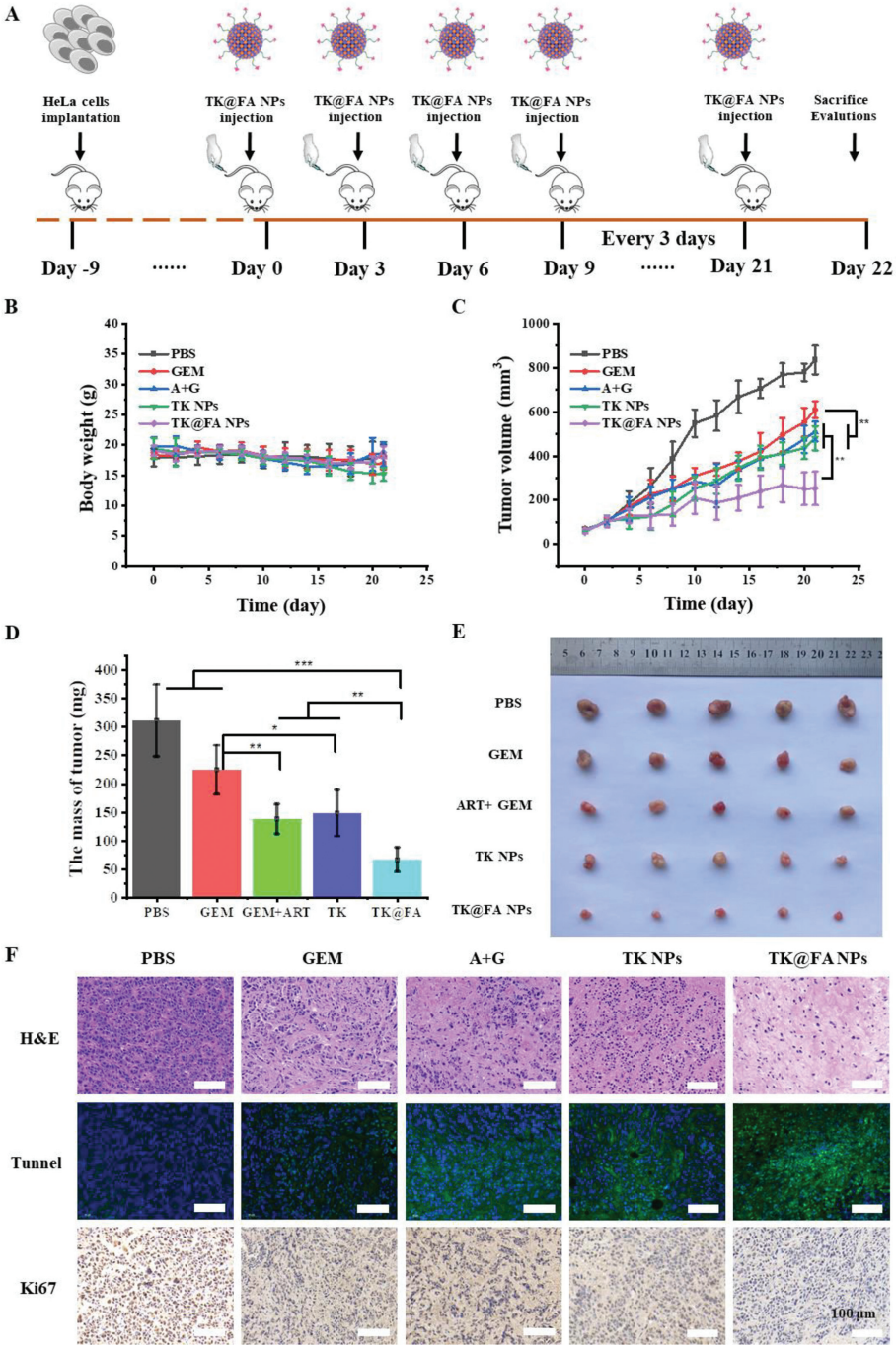

Fig. 3. *In vivo* antitumor study. (A) Schematic illustration of *in vivo* antitumor efficacy of TK@FA NPs. (B) Body weight, (C) growth curves, (D) tumor weight and (E) photograph of HeLa tumor-bearing mice in each group ($n = 5$). (F) H&E (top panel), TUNEL (middle panel) and Ki67 (bottom panel) staining of tumor slices with various treatments. Blue signals: Hoechst dye H33342 (nuclear stain). Green signals: TUNEL-positive cells. $^{*}P < 0.05$, $^{**}P < 0.01$, $^{***}P < 0.001$.

chemical index test showed that TK NPs and TK@FA NPs had good biocompatibility (Figs. S8 and S9 in Supporting information). Moreover, the hematoxylin-eosin staining (H&E) images of major organs were obtained and no distinct histopathological damage was observed (Fig. S10 in Supporting information), demonstrating that TK@FA NPs had good biocompatibility in the treatment of cervical cancer.

Next, H&E, Ki-67 and terminal deoxynucleotidyl transferase mediated dUTP nick-end labeling (TUNEL) staining were used to evaluate the proliferation and apoptosis of HeLa cells. As shown in Fig. 3F, necrotic tumor cells were found in the TK@FA NPs group, and the significant apoptosis of HeLa tumor cells in the TK@FA NPs group were also observed. From what had been discussed above, TK@FA NPs had good inhibitory effect on tumor cell proliferation and good potential to enhance the antitumor effect of Food and Drug Administration (FDA) approved chemical drug of GEM, promoting the transformation and application of nanomedicine.

In conclusion, the ROS responsive and ROS self-supplied prodrug (ART-TK-GEM) that could release the original active drug (ART and GEM) was prepared and the nano-formulation of the prodrug showed better antitumor effect than free drug combination (ART+GEM) in cervical cancer tumor-bearing mouse model. Notably, the ART not only inhibits the proliferation of tumor cells by the ROS produced by itself, but also increases the expression

of HO-1 and then decreases the expression of CDA to optimize metabolic pathways of GEM and improve the antitumor effect of GEM, attaining enhanced synergistic chemotherapy. The FA targeting group endows TK@FA NPs with stronger tumor tissue enrichment ability and makes TK@FA NPs obtaining enhanced inhibition of cell proliferation than other groups including the free drug combination (ART+GEM). The TK@FA NPs with responsive drug release characteristic and synergistic chemotherapy would provide a new opportunity to obtain more effective drugs based on FDA approved drugs for the treatment of cervical cancer. In this study, ART was introduced to realize the nanocrystalization of GEM, optimize the metabolic pathway of GEM and enhance the activity of GEM. Vector free and the use of clinically approved drugs to overcome the shortcomings of existing drugs will help accelerate the clinical research and commercial transformation of drugs, and promote the rapid development of nanomedicine. Strategic use of clinically approved drugs to improve the insufficiency clinical drug to realize new utilization of old drugs may be a new approach to drug discovery.

Declaration of competing interest

The authors declare that they have no known competing financial interests or personal relationships that could have appeared to influence the work reported in this paper.

Acknowledgments

We are grateful for financial support from Guangdong Nature Resource Center (GDNRC, No. (2020)037) and Natural Science Foundation of Guangdong Province (Nos. 22019A1515011498, 2019A1515011619).

Supplementary materials

Supplementary material associated with this article can be found, in the online version, at doi:10.1016/j.cclet.2023.108184.

References

[1] J. Ouyang, A. Xie, J. Zhou, et al., Chem. Soc. Rev. 51 (2022) 4996–5041.
[2] X. Shan, X. Gong, J. Lia, et al., Acta Pharm. Sin. B 12 (2022) 3028–3048.
[3] D.Y. Hou, M.D. Wang, N.Y. Zhang, et al., Nano Lett. 22 (2022) 3983–3992.
[4] S. Wang, J. Li, Z. Ye, et al., Colloids Surf. A 574 (2019) 44–51.
[5] Z. Li, Q. Xu, X. Lin, et al., Chin. Chem. Lett. 33 (2022) 1875–1879.
[6] Y.C. Zhang, L. She, Z.Y. Xu, et al., Chin. Chem. Lett. 33 (2022) 3277–3280.
[7] L.H. Liu, X.Z. Zhang, Prog. Mater. Sci. 125 (2022) 100919.
[8] S. Karaosmanoglu, M. Zhou, B. Shi, et al., J. Control. Release 329 (2021) 805–832.
[9] R. Liu, C. Luo, Z. Pang, et al., Chin. Chem. Lett. 34 (2023) 107518.
[10] Y. Yang, S. Zuo, J. Zhang, et al., Nano Today 44 (2022) 101480.
[11] Q. Wang, C. Wang, S. Li, et al., Chem. Mater. 34 (2022) 2085–2097.
[12] A. Çapcı, L. Herrmann, H.M.S. Kumar, T. Fröhlich, S.B. Tsogoeva, Med. Res. Rev. 41 (2021) 2927–2970.
[13] X. Dong, R.K. Brahma, C. Fang, S.Q. Yao, Chem. Sci. 13 (2022) 4239–4269.
[14] Y. Zhang, H. Cui, R. Zhang, H. Zhang, W. Huang, Adv. Sci. 8 (2021) 2101454.
[15] J. Xiang, X. Liu, G. Yuan, et al., Adv. Drug Deliv. Rev. 179 (2021) 114027.
[16] D.H. Zhao, C.Q. Li, X.L. Hou, et al., ACS Appl. Mater. Interfaces 13 (2021) 55780–55789.
[17] S. Wang, Z. Zhao, J. Yao, et al., Chin. Chem. Lett. 34 (2023) 107805.
[18] M. Scaranti, E. Cojocaru, S. Banerjee, U. Banerji, Nat. Rev. Clin. Oncol. 17 (2020) 349–359.
[19] Y. Zhua, J. Feijena, Z. Zhong, Nano Today 18 (2018) 65–85.
[20] R. Zhao, B. Wang, X. Yang, et al., Angew. Chem. Int. Ed. 55 (2016) 5225–5229.
[21] M. Wang, Z. Guo, J. Zeng, et al., Chin. Chem. Lett. 34 (2023) 107651.
[22] F.G. Ye, C.G. Song, Z.G. Cao, et al., Cancer Res. 75 (2015) 1504–1515.
[23] E. Moysan, G. Bastiat, J.P. Benoit, Mol. Pharm. 10 (2013) 430–444.
[24] H. Meng, M. Wang, H. Liu, et al., ACS Nano 8 (2015) 3540–3557.
[25] K.K. Frese, A. Neesse, N. Cook, et al., Cancer Discov. 2 (2012) 260–269.
[26] I.M. Ahmad, A.J. Dafferner, K.A. O'Connell, et al., Cancers 13 (2021) 2264 Basel.
[27] H. Sun, L. Yan, R. Zhang, et al., Biomater. Sci. 9 (2021) 5000–5010.
[28] S. Yang, D. Zhang, N. Shen, et al., J. Cell. Biochem. 120 (2019) 634–644.
[29] S. Wang, A. Wang, Y. Ma, et al., Biomater. Sci. 9 (2021) 774–779.
[30] L. Yu, Z. Wang, Z. Mo, et al., Acta Pharm. Sin. B 11 (2021) 2004–2015.
[31] H. Li, Y. Chen, T. Chen, et al., NPG Asia Mater. 9 (2017) e423.
[32] L. Huang, Y. Luo, X. Sun, et al., Biosens. Bioelectron. 92 (2017) 724–732.
[33] T. Efferth, Semin. Cancer Biol. 46 (2017) 65–83.
[34] Q. Li, Q. Ma, J. Cheng, et al., OncoTargets Ther. 14 (2021) 2563–2573.
[35] T. Efferth, Biochem. Pharmacol. 139 (2017) 56–70.
[36] G. Ren, D. Duan, G. Wang, et al., Colloids Surf. B 217 (2022) 112614.
[37] Y. Hao, Y. Chen, X. He, et al., Adv. Sci. 7 (2020) 2001853.
[38] M. Jiang, J. Mu, O. Jacobson, et al., ACS Nano 14 (2020) 16875–16886.
[39] S. Dalin, M.R. Sullivan, A.N. Lau, et al., Cancer Res. 79 (2019) 5723–5733.